Electronic Supplementary Material (ESI) for RSC Advances.
This journal is © The Royal Society of Chemistry 2015

Supporting Information

Mechanically exfoliated g-C_3N_4 thin nanosheets by ball milling as high performance photocatalysts

Kaixing Zhu,[a] Wenjun Wang,[b] Alan Meng,[c] Meng Zhao,[b] Junhu Wang,[d] Mei Zhao,[d] Dongliang Zhang,[a] Yuping Jia,[b] Chunhua Xu[b] and Zhenjiang Li [e†]

a. College of Electromechanical Engineering, Qingdao University of Science and Technology, Qingdao, 266061, Shandong, P. R. China

b. Research & Development Centre for Functional Crystals, Institute of Physics, Chinese Academy of Sciences, Beijing 100190, Beijing, P. R. China

c. College of Chemistry and Molecular Engineering, Qingdao University of Science and Technology, Qingdao 266042, Shandong, P. R. China

d. College of Material Science and Engineering, Qingdao University of Science and Technology, Qingdao 266042, Shandong, P. R. China

e. Key Laboratory of Polymer Material Advanced Manufacturing Technology of Shandong Provincial, Qingdao University of Science and Technology, Qingdao 266061, Shandong, P. R. China

† Corresponding author. Tel.: +86 532 88956228; fax: +86 532 88956228. E-mail address: zhenjiangli@qust.edu.cn

1. AFM analysis

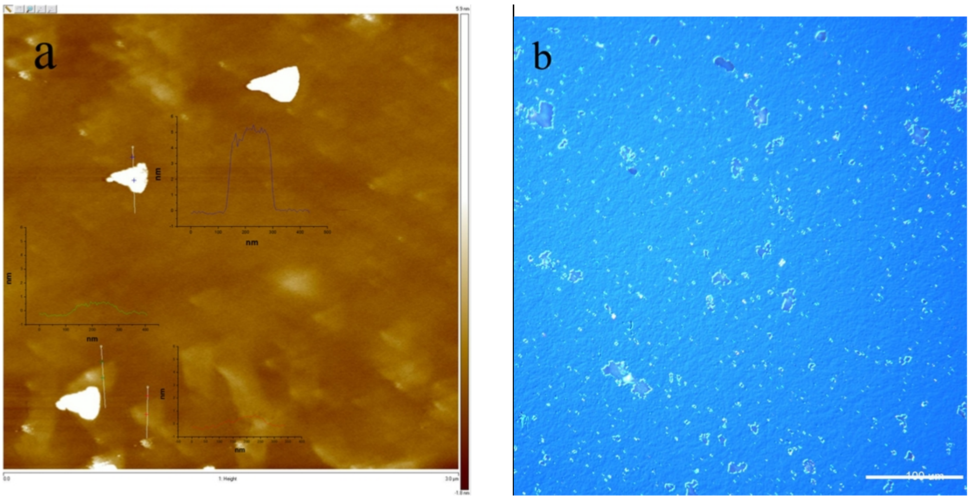

Figure S1. AFM image of the exfoliated g-C_3N_4 nanosheets (a) and the optical image of pristine bulk g-C_3N_4 particles.

AFM characterization was carried to extract the real thickness of the exfoliated nanosheets. As shown in Fig. S1, the randomly measured nanosheets are nearly the same thickness (0.5~5nm), indicating the exfoliated nanosheets are comprised of only several C-N layers. The very thin character of the exfoliated nanosheets in the AFM analysis matches well with the apparent feature in the TEM image in Fig. 3b. Optical image in Fig. S2 indicates that sizes of the bulk g-C_3N_4 particles are much larger than the exfoliated nanosheets with particles diameters in the range of 0.5~20 μm. Based on existing characterizations like XRD, TEM, and AFM, reduction in sizes and layers surely happened, making the enlargement of specific surface area quite reasonable. In addition, previous studies usually suggest a steady surface area increase with extended ball milling hours [SR1-3].

2. The mechanism for the enhancement of the photocatalytic performance

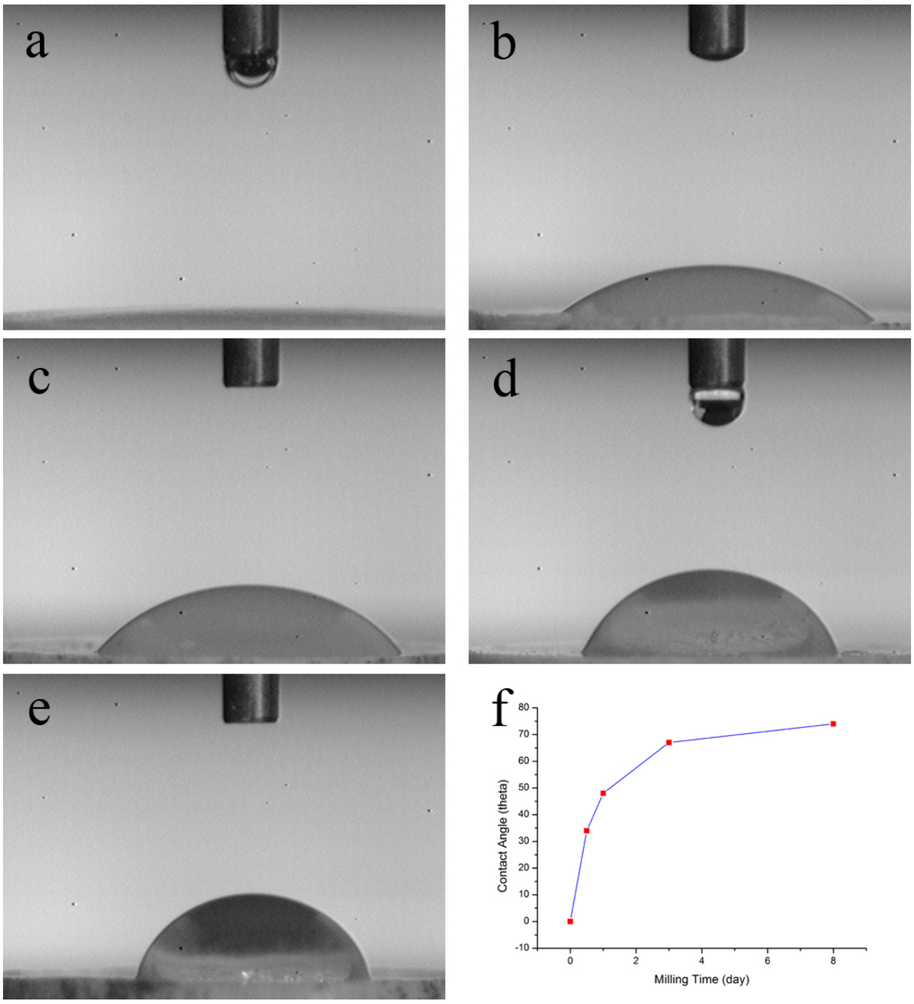

Figure S2. Photographs of water droplet shape and the corresponding contact angle plot.

In order to investigate the mechanism of the improvement, we have carried out the wettability test as shown in Fig. S2. When the droplet was dropped onto the surface of the pristine bulk g-C_3N_4 (Fig. S2a), the vast majority of the water droplet was imbibed and the rest spread across the surface with the relative CA about 0º, indicating that the pristine bulk g-C_3N_4 was hydrophilic. As shown in Fig. S2b-2e, when the ball milling time increases, CA of the sample increased steadily from 0º to 74º, which showed reduced hydrophilic property. Obviously, the ball milling process had a remarkable influence on the wettability of g-C_3N_4.

As well known, the wetting behavior of a solid surface is one of the most important aspects of surface physical chemistry, which affects the interaction process between a surface and its surrounding species. According to Cassie's law [SR4], wettability is determined by both the chemical composition and the geometrical structure of solid surface. In other words, the transformation of wettability always comes along with some physical or chemical change of materials. In our cases, the wettability modification is closely related to the reduction in sizes and layers of the samples in the ball milling process. In fact, changes were not limited to the wettability, but also to properties such as electronic structure (bandgap) and specific surface area in the milling process, which all together have impacts, no matter positive or negative, on the efficiency of photocatalytic degradation. Specifically, some degree of decrease in hydrophilicity would promote the photocatalytic degradation reactions, similar to the condensation effect in the SERS research where substrates with hydrophobic surfaces would be more likely to contact with the analyte through repelling the H_2O molecules. However, absolute conversion of wettability from hydrophilic to hydrophobic, in our opinion, would be harmful, because absolutely hydrophobic solid surface would reduce the interfaces with the solution enormously. On the other hand, the increased bandgap as indicated by the blue-shifted intrinsic absorption edge would narrow the light absorption range, and is unfavorable for the enhancement of the photocatalytic activity in principle. Reduction in the sample sizes and layers, as confirmed by the TEM and AFM analysis (Fig. 3b and Fig. S1a), is advantageous for the improvement of the photocatalytic activity because of the enlargement of specific surface area. The final photoctalytic activity is influenced by many factors practically, including bandgap, wettability, surface areas, electron-hole recombination rate and so on. One single unfavorable property is not decisive in many cases. One typical example is TiO_2, which is not competitive in visible light absorption but still accepted as an excellent photocatalyst. In this case, advantages by the wettability and specific surface area change are believed to outperform the harmful impact of the bandgap enlargement, leading to a final improvement in the photocatalytic activity.

3. The optical absorption analysis

The physicochemical properties of nanostructured semiconductors are found to be strongly size dependent [SR5-6]. It is well known that the nano-scale systems show interesting physical properties such as increasing semiconductor bandgap [SR6]. As for g-C_3N_4, there have been reports on the size dependent light absorption shift. For example, Liu showed the obvious blue shift of the intrinsic absorption edge in the "oxgen-etch" exfoliated nanosheets with respect to the bulk g-C_3N_4 [SR7]. The reason for the enlarger bandgap can be attributed to the well-known quantum confinement effect by shifting the conduction and valence band edges in opposite directions. The basic physical phenomena of quantum confinement were believed as a result of changes in the density of electronic states [SR8].

4. The optical absorption analysis

When the crystallites of a material become smaller, typically less than 100 nm, they would have limited number of parallel diffraction planes and so they produce broadened diffraction peaks instead of a sharp peak. Lattice strain present in the sample which is very likely in our ball milling process is another cause of broadening of Bragg diffraction peaks. In 1918, Scherrer developed a formula relating the mean crystallite size, t, of a powder to the broadening, B_L, of its powder diffraction peaks, known as Scherrer equation:

$$B_L = \frac{K\lambda}{t\cos\theta}$$

Where θ is the usual Bragg angle, λ is the radiation wavelength, and K is a constant which is taken as 0.89 [SR9].

The second main source of peak broadening is strain, or more correctly inhomogeneous strain because homogeneous strain (compression) only bring out the shifting of the diffraction peak, from θ to $\theta+\delta\theta$, but not broadening. An approximate relationship relating the mean inhomogeneous strain, ε, to the peak broadening can be expressed in the following simple form:

$$B_\varepsilon = C\,\varepsilon\tan\theta$$

Where the value of the constant C depends on the strain nature assumptions and is typically ≈4 or 5.

People would feel like separating the effects of size and strain from the broadened diffraction pattern when they are both present simultaneously. Williamson-Hall method was developed to estimate the lattice strain and particle sizes in which the observed peak broadening B may be represented as

$$B=B_L+B_\varepsilon$$

Where B is the observed peak broadening, B_L and B_ε are the broadening due to particle size and lattice strain respectively. It is necessary to know that the instrumental broadening has been ignored here. For more precise calculation, this part of contribution needs to be taken into account. Based on previous equations, the total peak broadening B may be expressed as

$$B=\frac{K\lambda}{t\cos\theta}+C\varepsilon\tan\theta$$

Which can be written as

$$B\cos\theta=\frac{K\lambda}{t}+C\varepsilon\sin\theta$$

We see that by plotting Bcosθ versus sinθ we will obtain the strain component from the slope (Cε) and the size component from the intercept (Kλ/t). By substituting the peak width and relevant angles, the obtained ε is 0.0067 (C is taken as 5) and the sample size is about 8 nm. The contribution ratio for the broadening between particle size and strain is about 5.6, which means that the main contribution of the peak broadening comes from the reduction in sizes and layers.

Supporting Reference:

[1]A. H. Emami, M. Sh. Bafghi, J. Vahdati Khaki and A. Zakeri, The effect of grinding time on the specific surface area during intensive grinding of mineral powder, Iranian J. Mater. Sci. & Eng., 2009, 6: 30-36.

[2]Y. Chen, J. F. Gerald, L. T. Chadderton, and L. Chaffron, Nanoporous carbon produced by ball milling, App. Phys. Lett., 1999, 74: 2782-2784.

[3]N. Pierard, A. Fonseca, J. Colomer, C. Bossuot, J. Benoit, G. Tendeloo, J. Pirard, J. Nagy, Ball milling effect on the structure of single-walled carbon nanotubes, Carbon, 2004, 42:1691-1697.

[4]A. Cassie, and S. Baxter, Wettability of porous surfaces, Trans. Faraday Soc., 1944, 40:546-551.

[5]X. Chen, Y. Jun, K. Takanbe, K. Maeda, K. Domen, X. Fu, M. Antonietti, and X. Wang, Ordered mesoporous SBA-15 type graphitic carbon nitride: a semiconductor

host structure for photocatalytic hydrogen evolution with visible light, Chemistry of Materials, 2009, 21: 4093-4095.

[6]H. Lin, C. Huang, W. Li, C. Ni, S. Ismat Shah, Y. Tseng, Size dependency of nanocrystalline TiO2 on its optical property and photocatalytic reactivity ememplified by 2-chlorophenol, Applied Catalysis B: Environmental, 2006, 68: 1-11.

[7]P. Niu, L. Zhang, G. Liu, and H. Cheng, Graphene-like carbon nitride nanosheets for improved photocatalytic activities, Adv. Funct. Mater., 2012, 22:4976-4770.

[8]A. P. Alivisatos, Semiconductor cluster, nanocrystals, and quantum dots, Science, 1996, 271: 933-937.

[9]P. Scherrer, Bestimmung der Grösse und der Inneren Struktur von Kolloidteilchen Mittels Röntgenstrahlen, Nachrichten von der Gesellschaft der Wissenschaften, Göttingen, Mathematisch-Physikalische Klasse, 1918, 2: 98-100.